THE JOURNAL OF BIOLOGICAL CHEMISTRY VOL. 289, NO. 20, pp. 14030–14044, May 16, 2014
© 2014 by The American Society for Biochemistry and Molecular Biology, Inc. Published in the U.S.A.

Heterologous Src Homology 4 Domains Support Membrane Anchoring and Biological Activity of HIV-1 Nef*[S]

Received for publication, March 7, 2014, and in revised form, April 3, 2014 Published, JBC Papers in Press, April 4, 2014, DOI 10.1074/jbc.M114.563528

Miriam M. Geist[‡], Xiaoyu Pan[‡], Silke Bender[§], Ralf Bartenschlager[§1], Walter Nickel[¶1], and Oliver T. Fackler[‡1,2]

From the Department of Infectious Diseases, [‡]Integrative Virology and [§]Molecular Virology, University Hospital Heidelberg, 69120 Heidelberg, Germany and the [¶]Biochemistry Center, Heidelberg University, 69120 Heidelberg, Germany

Background: HIV-1 Nef is a membrane-associated protein that acts as viral pathogenicity factor.
Results: Nef function requires regulated membrane interactions along transport pathways to and from the plasma membrane.
Conclusion: Nef function is determined by dynamic anterograde and endocytic transport cycles.
Significance: Dynamic transport cycles provide the basis for the multifunctionality of Nef.

The HIV-1 pathogenicity factor Nef enhances viral replication by modulation of multiple host cell transport and signaling pathways. Nef associates with membranes via an N-terminal Src homology 4 (SH4) domain, and membrane association is believed to be essential for its biological functions. At which subcellular site(s) Nef exerts its different functions and how kinetics of membrane interactions contribute to its biological activity are unknown. To address how specific characteristics of Nef membrane association affect its biological properties, the SH4 domain of Nef was replaced by heterologous membrane targeting domains. The use of a panel of heterologous SH4 domains resulted in chimeric Nef proteins with distinct steady state subcellular localization, membrane association efficiency, and anterograde transport routes. Irrespective of these modifications, cardinal Nef functions affecting host cell vesicular transport and actin dynamics were fully preserved. In contrast, stable targeting of Nef to the surface of mitochondria, peroxisomes, or the Golgi apparatus, and thus prevention of plasma membrane delivery, caused potent and broad loss of Nef activity. These results support the concept that Nef adopts its active conformation in the membrane-associated state but exclude that membrane-associated Nef simply acts by recruiting soluble factors independently of its local microenvironment. Rather than its steady state subcellular localization or membrane affinity, the ability to undergo dynamic anterograde and internalization cycles appear to determine Nef function. These results reveal that functional membrane interactions of Nef underlie critical spatiotemporal regulation and suggest that delivery to distinct subcellular sites via such transport cycles provides the basis for the multifunctionality of Nef.

Nef is a myristoylated 25–34-kDa protein encoded by HIV-1, HIV-2, and SIV. Although dispensable for virus replication in cultured cells, Nef potently increases virus replication and thus serves as a pathogenicity factor that accelerates disease progression in the infected host (1–3). This role of Nef in AIDS pathogenesis is also supported by transgenic mice in which expression of Nef induces AIDS-like depletion of $CD4^+$ T lymphocytes (4, 5). Nef bears no enzymatic activity but rather mediates its functions through a large set of interactions with cellular proteins. By virtue of this adaptor function, Nef affects many central processes in HIV target cells. This includes modulation of cellular transport pathways leading to down-regulation of many receptors from the surface of infected cells, which, for example, prevents superinfection (CD4, CXCR4/CCR5) (6, 7) or cytotoxic T cell lysis (8, 9) of productively infected cells and enhancement of HIV-1 particle infectivity (10–13). HIV-1 Nef also modulates cellular signaling pathways such as the T cell receptor cascade in T lymphocytes by simultaneous modulation of vesicular transport and actin dynamics. These alterations modify the response of infected T lymphocytes to T cell receptor stimulation by blocking T cell receptor proximal signaling at the plasma membrane (PM)[3] while triggering a signaling cascade initiated at intracellular membranes (14–20). Induction of signaling cascades initiating at intracellular membranes results from the retargeting of active pools of the Src family kinase Lck from the PM to recycling endosomes and the *trans*-Golgi network (TGN) (16, 20–25). Together, these effects appear to induce an intermediate state of T cell activation that supports HIV replication but prevents activation-induced cell death (16, 26).

Approximately 10–30% of the total pool of Nef protein is membrane-associated at steady state and association with host cell membranes is generally assumed to represent a prerequisite for all individual Nef activities (27–32). Efficient membrane attachment of Nef requires cotranslational myristoylation at the glycine at position 2 (33–36). However, myristoylation alone confers only weak membrane attachment, and additional interactions are required for robust membrane binding (37–39). In case of Nef, this second signal consists of an arginine stretch (Arg^{17}-Arg^{19}-Arg^{21}-Arg^{22}). Myristoyl anchor and stretch of basic residues form an N-terminal membrane target-

* This work was supported by Deutsche Forschungsgemeinschaft TRR83 projects 5 (to W. N.), 13 (to R. B.), and 15 (to O. T. F.).
[S] This article contains supplemental Figs. S1–S3.
[1] Members of Cluster of Excellence CellNetworks EXC81.
[2] To whom correspondence should be addressed: Dept. of Infectious Diseases, Integrative Virology, University Hospital Heidelberg, Im Neuenheimer Feld 324, 69120 Heidelberg, Germany. Tel.: 49-6221-561322; Fax: 49-6221-565003; E-mail: oliver.fackler@med.uni-heidelberg.de.

[3] The abbreviations used are: PM, plasma membrane; MFI, mean fluorescence intensity; OT, organelle targeting; OTS, organelle targeting signal; SDF-1α, stromal cell-derived factor 1α; SH4, Src homology 4; TGN, *trans*-Golgi network; M fraction, membrane fraction; C fraction, cytosolic fraction.

ing module referred to as Src homology 4 (SH4) domain. SH4 domains are known to mediate membrane association of Src family kinases and are composed of variable combinations of acylation (myristoylation or palmitoylation) and basic residues. The Nef SH4 domain also contains two lysines at positions 4 and 7, which mediate lateral segregation of a subpopulation of membrane-bound Nef (~5% of total Nef) into raft-like membrane microdomains (30).

Although the N-terminal SH4 domain of Nef has been established as a key determinant for overall membrane association, it is unclear how the selectivity of Nef for specific cellular membranes is achieved. In addition to the abundant soluble cytoplasmic pool of Nef, the predominant subcellular localizations of the viral protein are the inner leaflet of the PM, as well as endocytic and perinuclear membrane vesicles. Consistent with the role of the basic stretch in the Nef SH4 domain for membrane targeting, *in vitro* binding of Nef to liposomes revealed a preference of Nef for negatively charged lipids but did not identify a requirement for a specialized lipid composition for membrane association (40). Because Nef more efficiently inserted into liposomes with high curvature, it remains unclear how specific targeting of Nef to and association with the PM is achieved in cells, and these findings suggest the involvement of specialized delivery pathways.

Despite this characterization of Nef-membrane interactions, many aspects on how this association is linked to the biological activities of Nef remain to be established. Nonmyristoylated G2A mutants of Nef are widely used to assess the relevance of membrane association for Nef function (11, 28–31, 41–44). Such mutants, however, retain significant residual membrane association, display reduced but not abrogated biological activity, and therefore do not allow drawing definite conclusions on the functional relevance of the overall membrane association of Nef. Given that Nef activities such as enhancing endocytosis of CD4 (6, 34) are exerted directly at the PM or affect composition and morphology of the cell surface (7, 9, 18, 19, 23, 25, 45), it is generally assumed that the PM is the predominant subcellular site of the biological activity of Nef. However, biologically active Nef subpopulations have not yet been visualized, and most Nef effects could also be explained by activities originating from other subcellular sites. How native Nef molecules are delivered to the PM has not been explored in detail. Our recent results suggest that Nef affects anterograde transport of specialized membrane microdomains with select SH4 domain cargo proteins (24), raising the possibility that its own PM transport regulates the biological activity of Nef. Finally, as exemplified for retargeting of Lck to recycling endosome/TGN compartments, Nef can trigger effects on intracellular vesicular transport at a distance, *i.e.* without its presence at the final destination of the affected cargo (16, 24). Taken together, the general assumption that Nef requires membrane association for its biological activity has not been rigorously assessed experimentally, and it is unclear where and how these interactions are regulated.

We employed here a heterologous targeting approach in which the SH4 domain of Nef was replaced with different membrane targeting domains. This resulted in a panel of chimeric Nef proteins with native topology throughout all intracellular sorting steps that displayed divergent segregation to membrane fractions, employed distinct anterograde transport routes, and localized to specific subcellular sites. The functional characterization of these constructs revealed that Nef activity does not depend on its extent of membrane association, its steady state subcellular localization, or the anterograde transport pathway used but critically requires dynamic vesicular transport passing by the PM.

EXPERIMENTAL PROCEDURES

Cell Lines, Reagents, and Plasmids—Jurkat TAg (Jurkat cells with the large T antigen of simian virus 40) (46) and Jurkat CCR7 cells were cultivated in RPMI 1640 supplemented with 10% FCS and 1% penicillin-streptomycin (all from Invitrogen). Jurkat CCR7 medium additionally contained 1× nonessential amino acids (Invitrogen), 1× sodium pyruvate (Invitrogen), 10 mM HEPES (pH 7.4) and 45.76 μM β-mercaptoethanol (Roth). HeLa and NIH 3T3 cells were cultivated in DMEM or DMEM (low glucose), respectively, supplemented with 10% FCS and 1% penicillin-streptomycin (all from Invitrogen). The following antibodies were used: anti-CD3 (clone HIT3a against CD3ε; BD Biosciences), mouse anti-Lck (clone 3A5; Santa Cruz), mouse anti-β-COP (kindly provided by Britta Brügger (47)), mouse anti-Cytc (BD Biosciences), rabbit anti-PMP70 (Abcam), mouse anti-transferrin receptor (Zymed Laboratories), mouse anti-myosin light chain (Sigma-Aldrich), mouse anti-GFP (Sigma-Aldrich), rat anti-GFP (Chromotek), sheep anti-Nef antiserum (gift from M. Harris, University of Leeds), and allophycocyanin-conjugated mouse anti-human CD4 (clone RPA-T4; BD Biosciences). Secondary goat anti-rabbit and anti-mouse Alexa Fluor 568 antibodies were purchased from Invitrogen. Poly-L-lysine and protease inhibitor mixture was purchased from Sigma-Aldrich. For F-actin staining, tetramethylrhodamineisothiocyanate-conjugated phalloidin was obtained from Sigma-Aldrich. The expression constructs for HIV-1 SF2 Nef WT and PalmNef fused to GFP, as well as the respective plasmid encoding for GFP, were described earlier (7, 48). The G2AKR mutant was generated by site-directed mutagenesis of the KR mutant (30) and was subcloned into the pEGFP-N1 vector. To obtain the chimeric SH4 domain and organelle targeting (OT) Nef.GFP constructs, nucleotides 1–66 of *nef* were replaced with nucleotides 1–54 of the corresponding SH4 domain-containing protein (amino acid sequences are shown in Fig. 1*A*) or the corresponding organelle targeting signals (OTSs), respectively. The OTS of Pex13 (49) was obtained by PCR using pEGFP-C1NLSopt_MAVS(CT)_Pex13TM as a template. The OTS of revGlc-NefΔSH4 consists of the transmembrane domain of galactosylgalactosylxylosylprotein 3-β-glucuronosyltransferase 2 in inverted orientation (amino acids 23–2) (50). For mitochondrial targeting, nucleotides 1–87 of the *TOM20* coding sequence were used. The lentiviral vector system containing vector plasmids pWPI or pWPXL, envelope plasmid pMD2.G (VSV-G) and packaging plasmid pPAX2 was purchased from Addgene. The expression enhancer plasmid pAdVAntage was purchased from Promega. The *nef wt* gene, as well as the genes for the different chimeric Nef proteins used in the membrane fractionation experiment, were inserted into pWPI or pWPXL, respectively, resulting in the according pWPI- or pWPXL-Nef.GFP expression plasmid.

Transfection of Cells—Jurkat TAg and Jurkat CCR7 cells (5×10^6 to 1×10^7) were transfected with 20–60 μg of total plasmid DNA via electroporation (950 microfarads, 250 V or 850 microfarads, 250 V, respectively; Bio-Rad GenePulser). Transfection of T cells results in Nef expression levels comparable with those in HIV-1-infected T cells (51), and Nef displays similar membrane association in transfected and infected cells (28–30). HeLa cells were plated in 6-well plates containing two cover glasses (Marienfeld) and transfected with 4 μg of plasmid DNA using Lipofectamine 2000 (Invitrogen). For live cell imaging, HeLa cells were plated in μ-Slide (chambered coverslips) 8 wells (ibidi) and transfected with 0.4 μg of plasmid DNA.

Lentiviral Vector Production and Transduction of Jurkat TAg Cells—Lentiviral vector stocks were generated by transfection of HEK293T cells with the according lentiviral vector and packaging plasmids. Twenty-four hours before transfection, 5×10^6 293T cells were seeded per 15-cm dish. Transfection was performed using JetPEI transfection reagent (Peqlab) according to the manufacturer's recommendations using: 22.5 μg of pWPXL vector plasmid with the according gene, 8 μg of envelope plasmid pMD2.G, 14.6 μg of packaging plasmid pPax2, 2.3 μg of pAdvantage. The transfection mix was directly added to the medium, and a medium exchange was performed after 4–6 h. Virus supernatant was harvested after 48 or 72 h, filtrated using 0.22-μm-pore size radio-sterilized filters, concentrated by ultracentrifugation, and stored at −80 °C. The virus supernatant was titrated on Jurkat TAg cells to calculate the amount of supernatant necessary to reach transduction efficiency between 35 and 90% for the membrane fractionation experiment. For transduction, 2×10^6Jurkat TAg cells/well were mixed with the according amount of virus supernatant in 24-well plates, the cells were spin-infected for 90 min at 2,000 rpm at room temperature and cultivated for 17–20 h at 37 °C before additional medium was added. Membrane fractionation experiments were performed 72 h after transduction. Nef expression levels in T lymphocytes are similar following transduction with retroviral vectors or infection with HIV-1 (52).

Immunofluorescence Analyses—For T cells, microscope cover glasses (Marienfeld) were prepared by incubation in 0.01% poly-L-lysine (Sigma-Aldrich) solution at room temperature for 10 min. Cells were plated on the cover glasses, incubated for 5 min, and subsequently fixed for at least 15 min, by directly adding PBS-3% paraformaldehyde. For NIH 3T3 cells, the cells were fixed with PBS, 3% paraformaldehyde after the indicated time points postmicroinjection. After permeabilization with PBS, 0.1% Triton X-100 for 1–5 min, the cells were blocked with PBS, 1% bovine serum albumin for 30 min. Stainings and protocols for the Lck retargeting and lymphocyte ruffling assay were described previously (19, 24). Samples were analyzed by confocal laser scanning microscopy (LSM 510; Zeiss) using a 100× oil immersion objective lens. Confocal stacks of F-actin in Jurkat TAg cells were acquired using a Leica DM IRE2 microscope with a 63× oil immersion objective lens. Images were processed with ImageJ and Adobe Photoshop CS3.

Membrane Fractionation—Subcellular fractionation was performed using slight modifications of a previously described protocol (30). Briefly, Jurkat TAg cells were transduced with lentiviral vectors encoding for the different Nef.GFP fusion proteins (transduction efficiency, 35–90%). Seventy-two hours post-transduction, the cells were lysed in 600 μl of TNE buffer (50 mM Tris-HCl, pH 7.4, 150 mM NaCl, 5 mM EDTA, and protease inhibitor mixture) for 20 min on ice, homogenized with a Dounce homogenizer, and loaded on an Optiprep (Invitrogen) gradient (350 μl of cell lysates were mixed with 600 μl of 60% Optiprep and overlaid with 2.5 ml of 28% Optiprep and 600 μl of TNE), followed by ultracentrifugation (35,000 rpm, 3 h, 4 °C). Eight fractions of 500 μl each were collected from the top. Fraction 2, which represented the membrane (M) fraction, and the soluble cytosolic (C) fractions 7 and 8 were used for Western blot analysis. Transferrin receptor and myosin light chain served as markers for M and C fractions, respectively.

Western Blotting—Washed cell pellets were lysed in SDS lysis buffer. Proteins were separated on 10–12% (expression of constructs) or 11% (membrane fractionation) SDS-PAGE and blotted to nitrocellulose membranes. Blocked membranes were probed with the following primary antibodies: mouse anti-transferrin receptor (Zymed Laboratories), mouse anti-myosin light chain (Sigma-Aldrich), mouse anti-GFP (Sigma-Aldrich), rat anti-GFP (Chromotek), sheep anti-Nef antiserum (gift from M. Harris, University of Leeds). Secondary antibodies were conjugated to horseradish peroxidase for ECL-based detection. For detection of Nef.GFP fusion proteins with the Odyssey® infrared imaging system (LI-COR Biosciences), the secondary antibody was labeled with IRDye® 800 (Rockland).

Western Blotting Quantification—The relative distribution of the various Nef.GFP fusion proteins between M and C fractions was determined by scanning Western blot membranes with the LI-COR imaging system that measures the infrared fluorescent signal emitted by the IRDye® 800 conjugated to the secondary antibody. Signals were quantified using the Odyssey software (Odyssey® infrared imaging system; LI-COR Biosciences) following background subtraction. Each fraction was first individually quantified, and the combined total signal from all fractions was then set to 100%. The values obtained for the individual M and C fractions for a given protein were then set relative to this 100%. The quantification shown in Fig. 3 represents the mean value of at least three independent membrane fractionation assays, quantified as described, with the corresponding standard deviations.

Microinjection—NIH 3T3 cells, which were grown on cover glasses, were microinjected into their nuclei with an AIS 2 microinjection apparatus using pulled borosilicate glass capillaries in principle as reported (45, 53). Plasmids encoding the indicated Nef.GFP fusion proteins were mixed in water at concentrations of 10 ng μl^{-1}. Following microinjection, cells were cultured for various times to allow protein expression and trafficking. At the indicated time points, cells were fixed with PBS, 3% paraformaldehyde and subjected to microscopic analysis. How the per cell Nef expression levels achieved by plasmid microinjection compare with those in HIV-1-infected cells is unclear. Hence, this approach was exclusively used to visualize anterograde transport of the first pools of newly synthesized protein at early time points postmicroinjection and thus limited protein expression.

Down-regulation of Cell Surface CD4—To quantify CD4 cell surface expression, Jurkat TAg cells were electroporated with

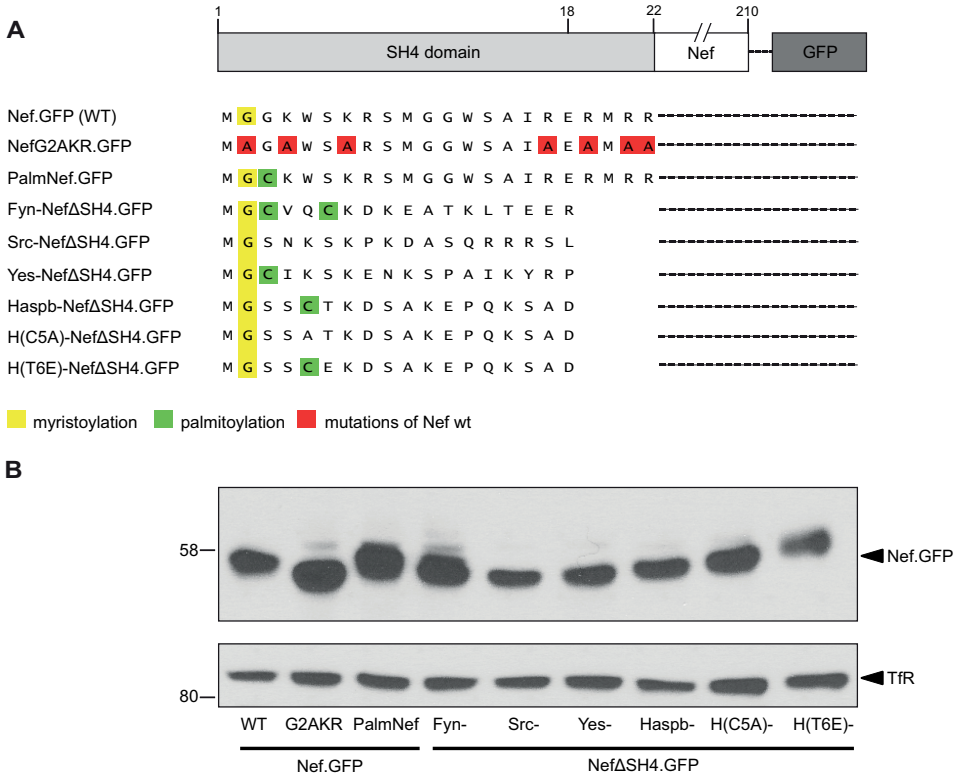

FIGURE 1. **Nef.GFP expression constructs containing different SH4 domains for heterologous targeting of Nef.** *A*, schematic representation of Nef.GFP constructs used in this project. To achieve heterologous targeting, the Nef SH4 domain was replaced by the shown SH4 domains. *B*, Western blot analysis of Jurkat TAg T lymphocytes transfected with the Nef.GFP expression constructs. Transferrin receptor served as loading control.

20 μg of expression plasmid, and 24 h post-transfection the cells were washed and stained in PBS with allophycocyanin-conjugated mouse-anti-human CD4 (clone RPA-T4) (BD Biosciences) antibody. A FACSCalibur with BD CellQuest Pro 4.0.2 software (BD Biosciences) was used for analysis, as well as the Cyflogic^{TM} software (CyFlo Ltd., Kyrkslätt, Finland). The mean fluorescence intensity (MFI) for surface-exposed receptors was quantified in principle as reported (7). Relative CD4 cell surface expression levels were normalized to the values obtained for control cells transfected with GFP expression vector (set to 100%).

RESULTS

Chimeric Nef.GFP Proteins Differ in Subcellular Localization and Membrane Association—To study how subcellular localization and membrane association of Nef.GFP, a functional analog of untagged Nef (7, 48, 51), affect its activities, we aimed at generating Nef.GFP variants with heterologous membrane targeting signals that would result in Nef proteins with membrane topology analogous to that of WT HIV-1 Nef. As negative control we sought to include a completely cytosolic Nef variant. Because Nef mutants constructed previously only lacked some of the residues described to contribute to Nef membrane association, we generated the mutant NefG2AKR.GFP. NefG2AKR.GFP lacks myristoylation acceptor and arginine stretch, which mediate membrane binding of Nef as well as the dilysine motif important for its detergent-resistant membrane association (Fig. 1*A*). For heterologous targeting, the SH4 domain of Nef was deleted (NefΔSH4) and replaced by SH4 domains of different Src family kinases, as well as the Haspb (hydrophilic acylated surface protein B) of *Leishmania* (Fig. 1*A*). The SH4 domains used for Nef retargeting display different acylation patterns and confer distinct subcellular localization, membrane affinity, and usage of intracellular transport routes in their native context. Although the SH4 domain of Src closely resembles that of Nef (*e.g.* identical acylation pattern) and can substitute for that of Nef in mediating incorporation into HIV particles (39), Fyn and Yes were included because they mediate efficient PM association in their native context. The SH4 domain of the *Leishmania* Haspb protein mediates similarly efficient PM targeting; however, introduction of C5A and T6E mutations results in retargeting to the Golgi and/or perinuclear endosomes (54). In addition to these SH4 domain chimeras, the previously described Nef.GFP mutant PalmNef, which is palmitoylated because of a G3C mutation and thus enriched in detergent-resistant membranes relative to WT Nef (48, 55), was included in our analysis. All chimeric Nef.GFP proteins were expressed at similar levels in Jurkat TAg T lymphocytes (Fig. 1*B*).

We next determined whether the heterologous SH4 domains fused to NefΔSH4.GFP affected the steady state subcellular distribution of the viral protein by confocal live cell imaging of transfected HeLa cells (Fig. 2*A*; see Fig. 2*C* for quantification). As described earlier (29, 30, 48, 56, 57) Nef.GFP displayed a distribution between PM, cytoplasm, and perinuclear region (*category 2*, *black bars* in Fig. 2*C*), and palmitoylation reduced the pool of apparently non-membrane-associated Nef.GFP in the cytoplasm (*category 3*, *dark gray bars* in Fig. 2*C*). These

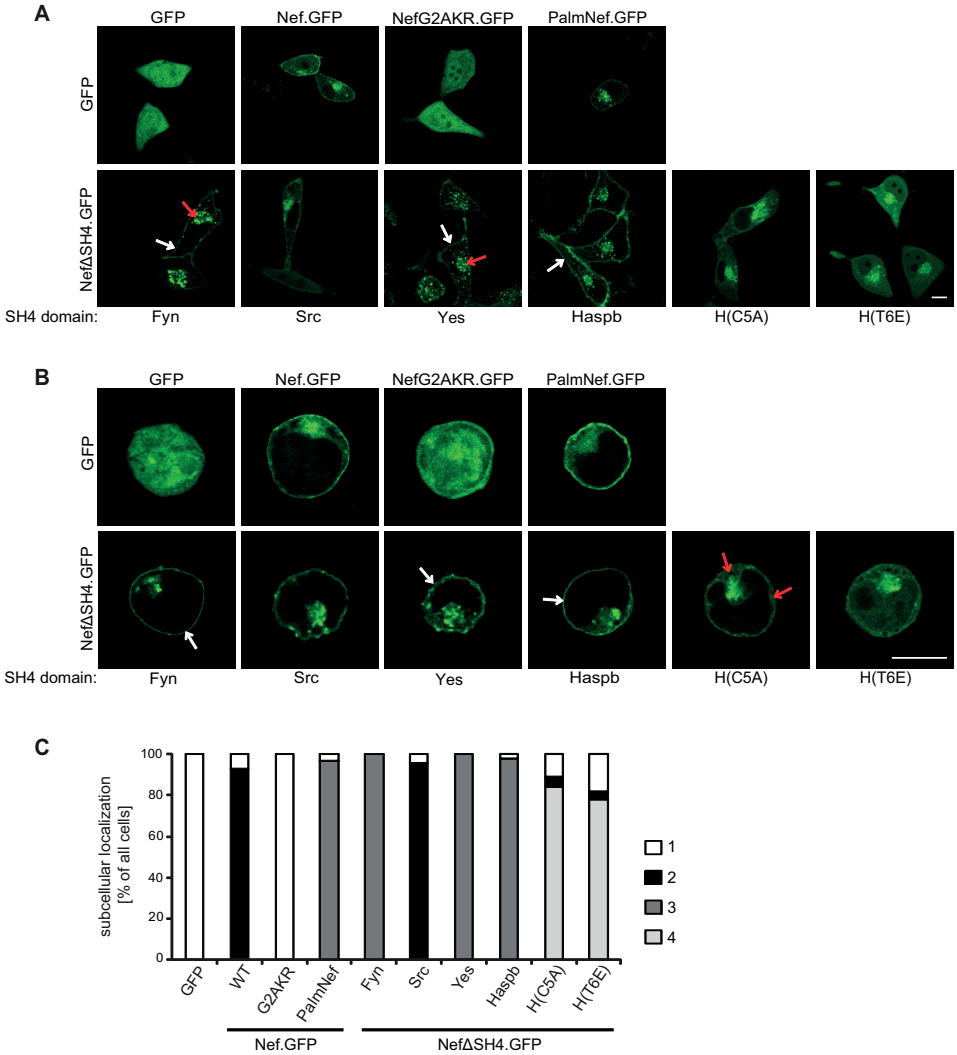

FIGURE 2. **Subcellular localization of chimeric Nef.GFP proteins in transfected cells.** *A*, live cell imaging of HeLa cells transiently expressing the indicated Nef.GFP proteins. Cells were analyzed by confocal microscopy 24 h post-transfection. Individual representative Z sections are shown. *Arrows* indicate localization at PM (*white arrows*) or strong intracellular accumulation (*red arrows*), respectively. *B*, transfected Jurkat TAg cells were plated on poly-L-lysine-coated cover glasses, fixed 24 h post-transfection, and analyzed by confocal microscopy. Individual representative Z sections are shown. *Arrows* indicate localization at PM (*white arrows*) or in the cytoplasm (*red arrows*), respectively. *Scale bar*, 10 μm. *C*, quantification of the frequency of transfected HeLa cells displaying the following subcellular localizations: *category 1* (*white bars*), cytoplasm; *category 2* (*black bars*), cytoplasm, intracellular accumulation, PM; *category 3* (*dark gray bars*), intracellular accumulation, PM; *category 4* (*light gray bars*), cytoplasm, intracellular accumulation. HeLa cells transfected with the different Nef.GFP expression plasmids were grown on cover glasses and fixed 24 h post-transfection. At least 100 cells were analyzed per condition.

subcellular distributions were markedly distinct from that of NefG2AKR.GFP, which localized diffusely throughout the nucleus and cytoplasm and which was indistinguishable from that of GFP alone (category 1, *white bars* in Fig. 2*C*). Heterologous exchange of the Nef SH4 domain had different effects on the subcellular distribution of the viral protein, depending on the individual SH4 domain used. Src-NefΔSH4.GFP displayed a subcellular distribution similar to Nef.GFP. In contrast, Fyn- and Yes-NefΔSH4.GFP showed clear PM association and stronger perinuclear accumulation than Nef.GFP, and virtually no signal was detected in the cytoplasm (Fig. 2*A*, indicated by *white* or *red arrows*, respectively; *category 3*, *dark gray bars* in Fig. 2*C*). Similarly, strong PM association was observed for Haspb-NefΔSH4.GFP (Fig. 2*A*, indicated by *white arrow*). Consistent with previous findings (54), H(C5A)- and H(T6E)-NefΔSH4.GFP localized to intracellular compartments but also diffusely to the cytoplasm, as well as faintly to the PM (*category 4*, *light gray bars* in Fig. 2*C*). To validate the specific and distinct subcellular localization of these SH4-Nef.GFP chimeras in HIV target cells, the proteins were expressed and analyzed in Jurkat TAg T lymphocytes post fixation (Fig. 2*B*). The results obtained essentially confirmed the results gained with live HeLa cells with the SH4 domains of Fyn, Yes, and Haspb mediating enhanced PM association of Nef.GFP and a redistribution to cytoplasm and intracellular membranes by the Haspb SH4 domain mutants (Fig. 2*B*, indicated by *white* or *red arrows*, respectively).

In addition to the visualization of Nef.GFP distribution in individual cells, we sought to obtain quantitative information on the overall membrane association of the chimeric Nef.GFP proteins. Membrane fractionations were conducted of 4.8–5 $\times$ 10^7 Jurkat TAg cells following efficient transduction with lentiviral vectors encoding for our panel of SH4-Nef.GFP chimeras. Cell lysates were fractionated by ultracentrifugation

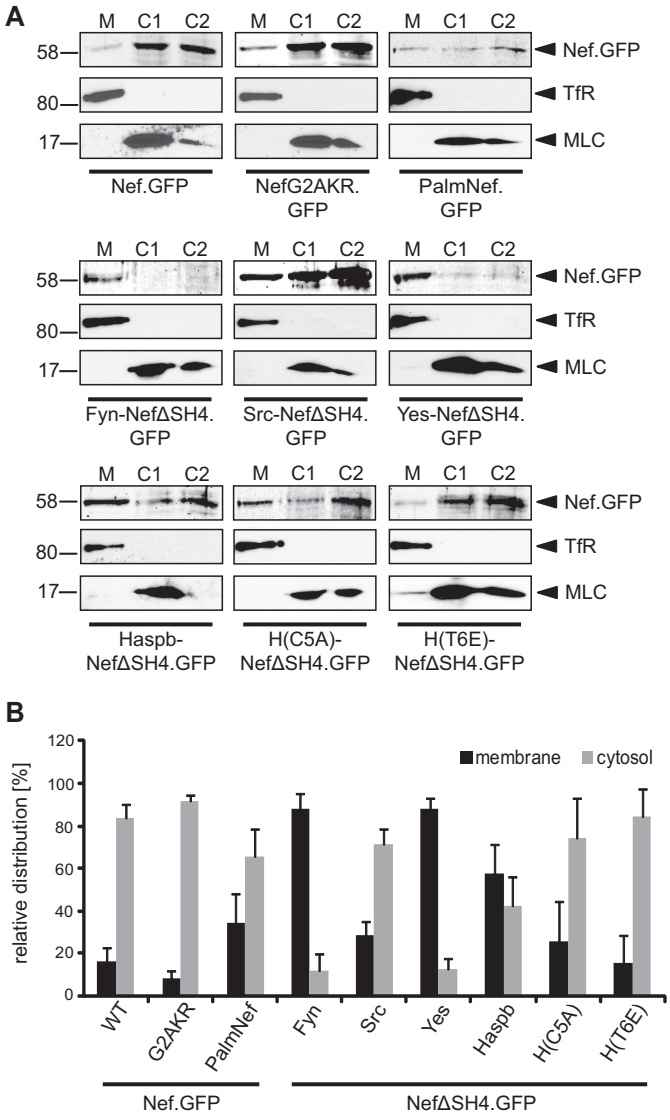

FIGURE 3. **Membrane association of chimeric Nef.GFP proteins in transduced Jurkat TAg cells.** *A*, membrane fractionation of Jurkat TAg cells transduced with lentiviral vectors encoding for the indicated Nef.GFP proteins. Seventy-two hours post-transduction, cell lysates were fractionated into membrane (*M*) and cytosolic (*C1* and *C2*) fractions and analyzed by Western blotting for the distribution of Nef.GFP. Transferrin receptor (*TfR*) and myosin light chain (*MLC*) proteins were analyzed as markers for M and C1/C2 fractions, respectively. *B*, quantification of the membrane fractionation analysis presented in *A*. Shown is the relative distribution of the various Nef.GFP proteins into M and C1/C2 fractions with the total signal from both fractions set to 100%. The data represent average values from at least three independent experiments with the indicated standard error of the mean.

through an iodixanol gradient, and the membrane fraction 2 (M) and soluble cytoplasmic fractions 7/8 (C1/C2) were analyzed by Western blotting (30) (Fig. 3*A*; see Fig. 3*B* for quantification). Consistent with previous reports that detected 10–30% of total Nef protein associated to membranes (28–30, 39, 58, 59), ~16% of Nef.GFP was found in the membrane fraction. Palmitoylation significantly enhanced its membrane association (PalmNef.GFP, 35%), even though PalmNef.GFP was markedly less stable in the course of the membrane fractionation procedure than all other Nef.GFP proteins analyzed. Despite the lack of all described membrane contacts, NefG2AKR.GFP retained considerable association with membrane fractions (approximately 8%), which was only reduced to 50% of that of Nef.GFP (Fig. 3, *A* and *B*) and thus is comparable with NefG2A (28–30). Residues outside the Nef N terminus therefore contribute to its association with membrane fractions, possibly by interaction with membrane-bound proteins rather than by membrane insertion. This analysis also revealed that the different SH4 domains differentially influenced the segregation of Nef.GFP to the membrane fraction: although the Src SH4 domain mediated membrane association similar to PalmNef (28% of total Nef protein in M), Fyn and Yes SH4 domains shifted virtually all detectable Nef.GFP to the membrane fraction (~88% of total Nef protein in M). Redistribution into the membrane fraction was also enhanced by the SH4 domain of Haspb. Despite the different subcellular distribution, the Haspb SH4 domain mutant T6E mediated segregation into the membrane fraction with similar efficiency as Nef.GFP (15%), whereas the Haspb SH4 domain mutant C5A provided slightly stronger membrane association (26%). Together these results demonstrate that the heterologous membrane targeting approach resulted in chimeric SH4-Nef.GFP proteins that mirror in subcellular localization and membrane association the properties of the individual SH4 domain used.

Chimeric Nef.GFP Proteins Vary in Anterograde Transport—Because the SH4 domains of different Src family kinases mediate PM delivery via distinct anterograde trafficking routes (60) and some Nef activities appear to be specific for specialized membrane microenvironment in this process (24), we next asked whether heterologous SH4 domain targeting affects the biosynthetic transport of Nef.GFP. For this analysis, we used an established plasmid microinjection approach that allows the visualization of PM transport of newly synthesized protein pools (45, 53). NIH3T3 cells were injected with Nef.GFP expression plasmids, and protein localization was analyzed at different time points within the first 3.5 h postinjection (Fig. 4). At 0.5 h, Nef.GFP and PalmNef.GFP were located exclusively to cytoplasmic vesicles distributed throughout the cell. Subsequently (1 and 3.5 h postmicroinjection), both proteins adopted their steady state localization (compare with Fig. 2) and were detected at the PM, as well as in the perinuclear area (Fig. 4, *A* and *B*). Nef.GFP and PalmNef.GFP thus are likely transported via the same anterograde pathway. In clear contrast, NefG2AKR.GFP was located diffusely throughout the whole cell at all time points and never appeared at the PM. Presumably reflecting the karyophilic properties of GFP in absence of specific targeting by Nef, NefG2AKR.GFP was also detected in the nucleus from 1 h postmicroinjection onwards. Consistent with the steady state localization, heterologous targeting of Nef.GFP by the Src SH4 domain did not have marked effects on the subcellular localization pattern during anterograde transport except that PM delivery of Src-NefΔSH4.GFP was more rapid and efficient than that of Nef.GFP (Fig. 4*B*). In contrast, Fyn-, Yes-, and Haspb-NefΔSH4, all of which showed pronounced membrane association and PM localization at steady state, were initially accumulated strongly in the perinuclear region (Fig. 4*A*, indicated by *arrows*). Moreover, Fyn-NefΔSH4.GFP was delivered to the PM with delay when compared with Nef.GFP (Fig. 4*B*) and did not reach its steady state distribution within the 3.5-h observation period, suggesting that in this case heterologous targeting routed Nef.GFP to a distinct anterograde

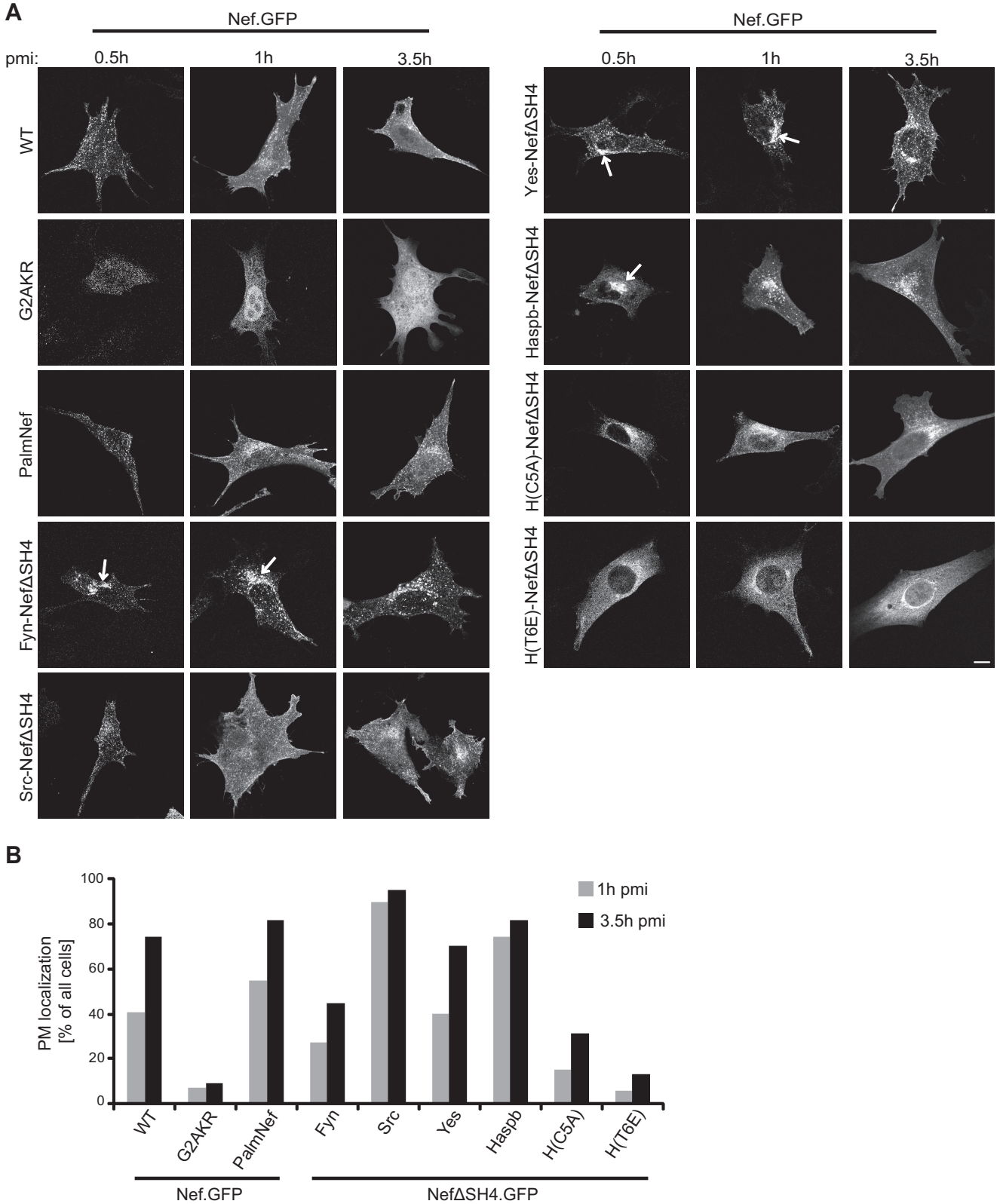

FIGURE 4. **Subcellular distribution of newly synthesized chimeric Nef.GFP proteins.** *A*, NIH 3T3 cells were microinjected with expression plasmids for the different chimeric Nef.GFP proteins and fixed at the indicated time points after microinjection. *pmi*, postmicroinjection. Cells were analyzed by confocal microscopy. Individual representative Z sections are shown. *Arrows* indicate different subcellular localization of Fyn-, Yes-, and Haspb-NefΔSH4 compared with Nef WT and Src-NefΔSH4. *Scale bar*, 10 μm. *B*, quantification of the frequency of cells displaying PM localization 1 and 3.5 h postmicroinjection of the indicated Nef.GFP proteins. At least 20 cells were analyzed per condition. The 0.5-h postmicroinjection time point was not quantified as low protein expression at this early point precluded thorough analysis.

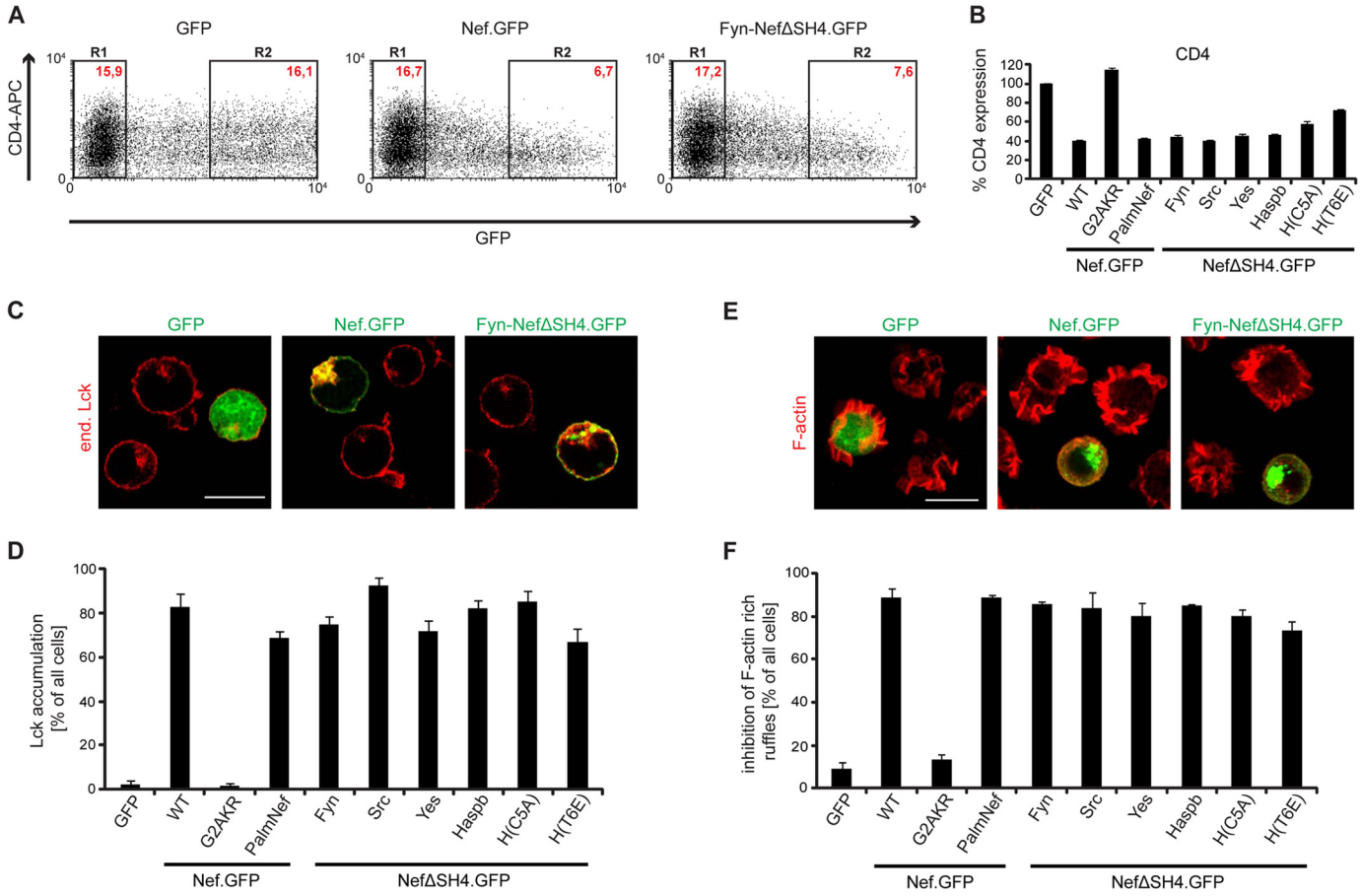

FIGURE 5. **Functional characterization of SH4 chimeric Nef.GFP proteins: down-regulation of cell surface CD4, Lck retargeting, and inhibition of F-actin ruffling.** *A*, CD4 cell surface expression in Jurkat TAg cells transfected with expression constructs for GFP, Nef.GFP, or Fyn-NefΔSH4.GFP. Twenty-four hours post-transfection, cells were stained for surface expression with allophycocyanin (*APC*)-conjugated antibodies against hm CD4 and analyzed by flow cytometry. *R1*, GFP-negative cells; *R2*, high level GFP expressing cells. *Red text*, MFIs of cells stained for CD4. *B*, down-regulation activity of the various chimeric Nef.GFP proteins. CD4 surface levels of GFP transfected cells were set to 100%. The data are means ± S.D. of at least three independent experiments. *C*, representative confocal pictures of Jurkat TAg cells transfected with expression constructs for GFP, Nef.GFP, or Fyn-NefΔSH4.GFP. Cells were plated on poly-L-lysine-coated cover glasses, fixed, and stained. Shown is a merge of endogenous (*end.*) Lck (*red*) and GFP (*green*). *Scale bar*, 10 μm. *D*, quantification of the frequency of cells displaying pronounced intracellular Lck accumulation. The data represent average values from three independent experiments ± S.D. with at least 100 cells analyzed per condition. *E*, representative maximum projections of confocal Z stacks of Jurkat CCR7 T cells transfected with expression constructs for GFP, Nef.GFP, or Fyn-NefΔSH4.GFP. Cells were plated on poly-L-lysine-coated cover glasses, stimulated with hm SDF-1α, fixed, and stained for F-actin using phalloidin-TRITC. Shown is a merge of F-actin (*red*) and GFP (*green*). *Scale bar*, 10 μm. *F*, quantification of cells that show full inhibition of F-actin ruffling. The data represent average values from three independent experiments ± S.D. with at least 100 cells analyzed per condition.

transport pathway. Expectedly, the C5A and T6E Haspb SH4 domain mutants also mediated initial targeting to perinuclear membranes (54). However, these constructs accumulated in the cytoplasm and were not abundantly detected at the PM within the time frame of observation. These results demonstrate that heterologous SH4 domain targeting alters the anterograde transport routes for PM delivery of chimeric Nef.GFP. Together, the heterologous SH4 domain targeting approach resulted in a panel of chimeric Nef.GFP proteins with divergent steady state subcellular localization, membrane association patterns, and anterograde transport pathways.

SH4 Chimeric Nef.GFP Proteins Retain Biological Activity—We next sought to analyze how heterologous SH4 domain targeting affects the biological activity of Nef.GFP. To assess down-regulation of the HIV entry receptor CD4 from the cell surface as one of the cardinal Nef functions, Jurkat TAg T lymphocytes were transfected with plasmids encoding for the different Nef.GFP chimeras, fluorescently stained for cell surface CD4, and analyzed by flow cytometry. The MFI for surface-exposed receptors was quantified as previously described (7). Relative CD4 cell surface expression levels were normalized to the values obtained for control cells expressing GFP (set to 100%), which showed no cell surface down-regulation of CD4 (Fig. 5, *A*, *left panel*, and *B*). Nef.GFP strongly down-regulated cell surface CD4 levels to ~40% of the control cells (Fig. 5, *A*, *middle panel*, and *B*). Despite its distinct subcellular localization, membrane association, and anterograde transport pathway, Fyn-NefΔSH4.GFP down-regulated CD4 levels from the cell surface with comparable efficiency to Nef.GFP (Fig. 5, *A*, *right panel*, and *B*). Similarly efficient CD4 down-regulation was observed with all other SH4 Nef.GFP fusion proteins (Fig. 5*B*) except H(C5A)- and H(T6E)-NefΔSH4.GFP, whose CD4 down-regulation was slightly reduced (58 or 72% cell surface CD4 remaining). Analysis of cell surface MHC-I down-regulation by Nef was precluded because the SH4 Nef chimera constructed lack the M20 residue required for this Nef activity (61–65); however, the analysis of chimeric Nef proteins containing heterologous SH4 domains in addition to the Nef SH4 domain

suggested that SH4 domain-mediated retargeting of Nef does not affect this Nef activity (data not shown).

We next assessed the ability of Nef to retarget endogenous Lck from the PM to endosomes and TGN in Jurkat TAg T lymphocytes transiently expressing the various Nef.GFP chimeras (15, 16). As expected, GFP or NefG2AKR.GFP had no influence on the intracellular localization of Lck that predominantly localized to the PM, with a small fraction residing in the perinuclear region (Fig. 5, *C*, *left panel*, and *D*; supplemental Fig. S1). In contrast, Nef WT induced a potent intracellular accumulation of Lck with only residual kinase at the PM remaining (Fig. 5*C*, *middle panel*). Retargeting of Lck similar to that observed with Nef WT was induced by all SH4 domain constructs (see image for Fyn-NefΔSH4.GFP in Fig. 5*C*; quantification in Fig. 5*D*; and supplemental Fig. S1).

Finally, we addressed the ability of SH4 Nef chimeras to inhibit actin remodeling in T lymphocytes, an activity that depends on molecular determinants distinct from those required for modulation of vesicular transport (19, 23, 25). Stimulation of T cells with the chemoattractant stromal cell-derived factor 1α (SDF-1α) induces the formation of pronounced F-actin-rich cell protrusions (ruffles), which are necessary for directional migration toward a chemokine gradient and the formation of which is inhibited by Nef (19). As expected, GFP and NefG2AKR.GFP expressing Jurkat CCR7 cells displayed pronounced actin ruffles in response to SDF-1α (Fig. 5, *E*, *left panel*, and *F*; and supplemental Fig. S2), whereas Nef WT potently suppressed the formation of F-actin ruffles (Fig. 5, *E*, *middle panel*, and *F*). Similar inhibition of F-actin ruffling was observed with all SH4 domain-containing Nef.GFP chimeras (Fig. 5, *E*, *right panel*, and *F*; and supplemental Fig. S2). Together these results establish that alterations in extent of membrane association, subcellular localization, and anterograde transport pathway used for PM delivery do not affect biological activities of Nef exerted by independent molecular determinants.

Heterologous Targeting of Nef.GFP to Specific Organelles—The above results demonstrated a surprising insensitivity of Nef to alterations in its subcellular localization, membrane segregation, and use of transport routes to the PM, whereas membrane association *per se* was essential for Nef activity. Given that Nef acts as adaptor protein to host cell machineries, these results were compatible with a scenario in which membrane-bound Nef recruits interacting cytosolic factors irrespective of its precise subcellular localization to modulate host cell processes. To test this hypothesis, we sought to stably target Nef to distinct cellular membranes while maintaining its topology as peripheral membrane protein that is anchored to membranes via its N terminus and is exposed to the cytoplasm. To this end, organelle-specific transmembrane domains were fused to the N terminus of NefΔSH4 to generate OT Nef.GFP chimeras (Fig. 6*A*). Targeting signals of TOM20 (66), Pex13 (49) or galactosylgalactosylxylosylprotein 3-β-glucuronosyltransferase 2 (50) were used for targeting of Nef to the outer membrane of mitochondria (TOM20-NefΔSH4.GFP), to peroxisomes (Pex13-NefΔSH4.GFP), or to the Golgi surface (revGlc-NefΔSH4.GFP), respectively. Expression levels of the OT Nef.GFP proteins in Jurkat TAg T lymphocytes were comparable with Nef WT (Fig. 6*B*). Live cell imaging of transfected HeLa cells (Fig. 6*C*) revealed that this heterologous organelle targeting approach was effective: revGlc-NefΔSH4.GFP localized to the perinuclear region, TOM20-NefΔSH4.GFP showed the tubular pattern typically observed for mitochondrial proteins (66, 67), and Pex13-NefΔSH4.GFP displayed a dot-like distribution within the cytoplasm consistent with targeting to peroxisomes. In fixed Jurkat TAg cells, the different OT Nef.GFP proteins showed subcellular localizations similar to those observed in live HeLa cells (Fig. 6*D*). The specificity of targeting to the respective organelle was confirmed by staining for organelle-specific marker proteins in fixed HeLa cells (Fig. 6*E*).

Stable Targeting of Nef to Membranes That Do Not Support PM Delivery Disrupts Nef Function—After having confirmed the specific subcellular distribution of the organelle-targeted Nef.GFP proteins, they were tested for their biological activity using the various functional assays described before. First, their ability to down-regulate CD4 molecules from the cell surface was analyzed. Consistent with the role of Nef as enhancer of CD4 internalization from the PM (68, 69), none of the OT Nef constructs showed any activity and were indistinguishable from the GFP control (Fig. 7, *A* and *B*). Considering that the ability of Nef.GFP to induce Lck retargeting from the PM to the perinuclear region does not require physical association or colocalization of the viral protein with the kinase (16, 24, 70), it was surprising that organelle targeting also compromised this activity (Fig. 7, *C* and *D*; and supplemental Fig. S3*A*). Although TOM20-NefΔSH4.GFP (Fig. 7, *C*, *right panel*, and *D*) completely lacked Lck retargeting activity, revGlc-NefΔSH4.GFP and Pex13-NefΔSH4.GFP induced moderate intracellular Lck in a minority of the cells analyzed (Fig. 7*D*). Consistently, none of the different OT Nef.GFP chimera showed efficient inhibition of F-actin ruffling upon stimulation with SDF-1α. Potently inhibited by Nef.GFP, TOM20-NefΔSH4.GFP failed to inhibit ruffle formation, and revGlc-NefΔSH4.GFP and Pex13-NefΔSH4.GFP only revealed moderate inhibition (Fig. 7, *E* and *F*; and supplemental Fig. S3*B*). The residual activity of revGlc- and Pex13-NefΔSH4.GFP was probably due to the slightly less efficient targeting compared with TOM20-NefΔSH4.GFP, which showed a clear and exclusive localization at mitochondria and was undetectable at any other subcellular site. Similar loss of function was observed for full-length Nef.GFP stably tethered to the cytoplasmic face of the endoplasmic reticulum (data not shown), excluding that organelle targeting of NefΔSH4.GFP caused functional defects specific for Nef proteins lacking their SH4 domain. Together, these results rule out that membrane-associated Nef acts by titrating out cytosolic factors but suggest that its various biological activities depend on specific interactions during its journey from biosynthesis to the PM and the endocytic/recycling transport machinery.

DISCUSSION

The goal of this study was to gain insight into how the strength and specificity of Nef-membrane interactions regulate the biological activities of the viral protein. Replacing the N-terminal membrane anchor of Nef with a series of heterologous SH4 domains resulted in stable Nef proteins that significantly differed in the anterograde transport pathway used, their steady

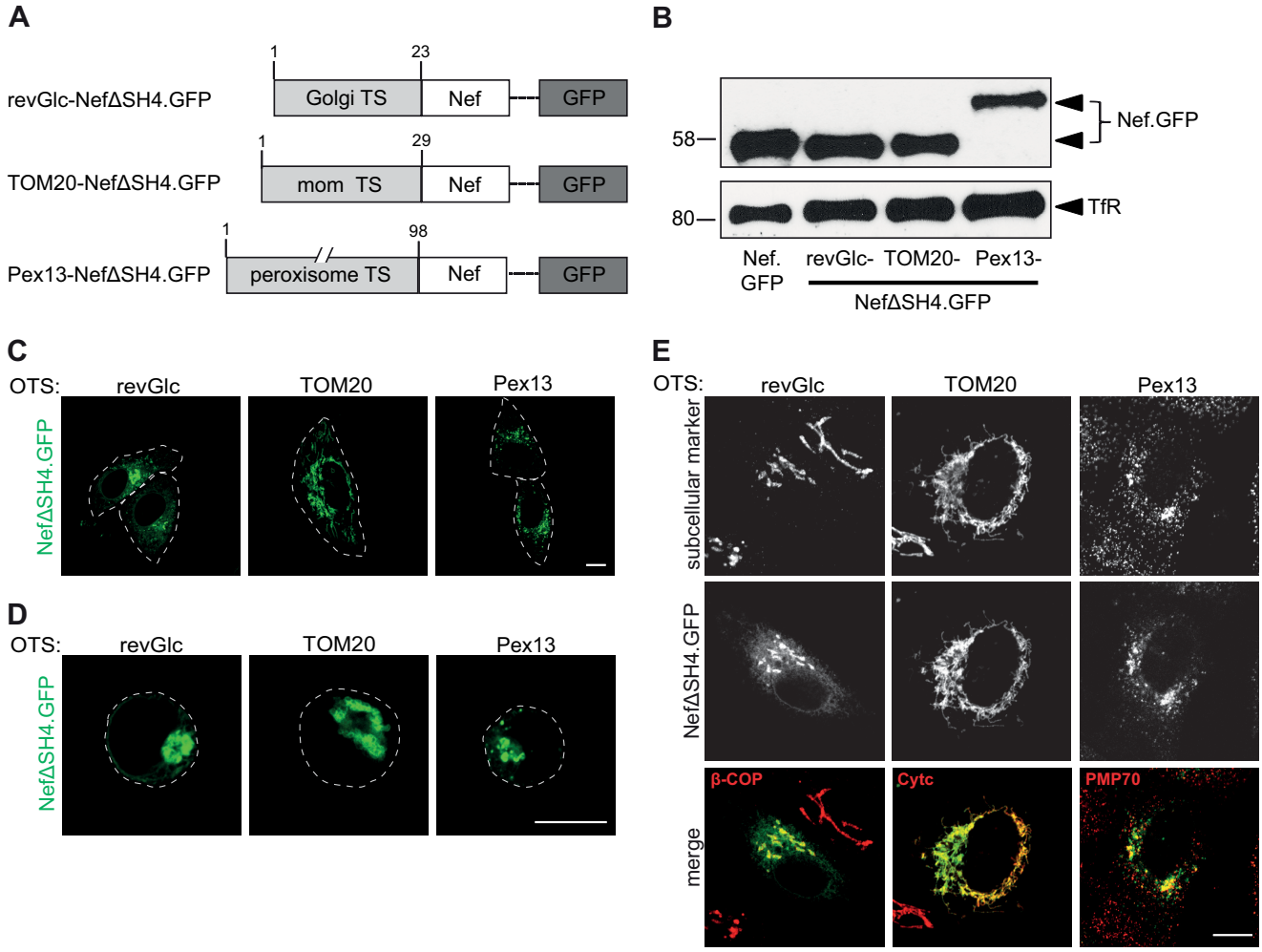

FIGURE 6. **Subcellular localization of Nef.GFP expression constructs containing different organelle targeting signals.** *A*, schematic representation of Nef.GFP constructs used. To achieve organelle specific targeting, the Nef SH4 domain was replaced by the shown targeting signals (TS). *mom*, mitochondrial outer membrane. *B*, Western blot analysis of transfected Jurkat TAg cells with the Nef.GFP expression constructs. Equal amounts of GFP positive cells were loaded per lane based on transfection efficiency (%). Transferrin receptor serves as loading control. *C*, live cell imaging of HeLa cells transiently expressing the indicated Nef.GFP proteins. Twenty-four hours post-transfection, cells were analyzed by confocal microscopy. Individual representative Z sections are shown. Cell circumferences are indicated by *gray dotted lines*. *D*, Jurkat TAg cells, transfected with the different Nef.GFP expression plasmids, were plated on poly-L-lysine-coated cover glasses, fixed 24 h post-transfection, and analyzed by confocal microscopy. Individual representative Z sections are shown. Cell circumferences are indicated by *gray dotted lines*. *E*, HeLa cells, transfected with the different Nef.GFP expression plasmids, were grown on cover glasses, fixed 24 h post-transfection, and stained for subcellular markers: β-COP (Golgi marker), Cytc (mitochondrial marker), or PMP70 (peroxisome marker), respectively, using fluorescently labeled antibodies. Shown is staining of the indicated subcellular marker (*red*), GFP (*green*), and the merge channel. Cells were analyzed by confocal microscopy. Individual representative Z sections are shown. *Scale bar*, 10 μm.

state subcellular localization, and the magnitude with which they segregated to membrane fractions. Despite these alterations, activities of Nef leading to modulation of host cell vesicular transport and actin dynamics remained entirely preserved. In contrast, tethering of Nef to the surface of unrelated organelles and thus prevention of PM delivery resulted in a broad and potent reduction of the biological activities of Nef. This characterization of HIV-1 Nef proteins targeted to membranes via various heterologous anchors provides several new insights into the relevance and regulation of Nef-membrane interactions. A first aspect relates to the overall requirement for membrane association for Nef activity. Based on the use of NefG2A or NefKR variants, it is generally assumed that membrane association is an essential prerequisite for the biological activities of Nef. Although these mutants lack important determinants for membrane association, they retain residual affinity to membrane fractions and display intermediate activity and thus do not allow drawing definite conclusions on the role of membrane association for Nef function (11, 28–31, 41–44). In contrast to these previously analyzed constructs, the Nef mutant NefG2AKR.GFP created herein lacks all known determinants for membrane association, is entirely defective in all tested Nef activities, and thus unambiguously supports the need for membrane association for Nef activity. Nevertheless, even NefG2AKR.GFP displayed residual membrane association as judged by membrane fractionation, presumably reflecting a biologically nonproductive interaction with membrane-bound proteins. Such residual membrane association of NefG2A.GFP or NefG2AKR.GFP cannot be appreciated by live cell imaging in which the prominent cytoplasmic pools likely prevent the detection of low abundant membrane-associated pools.

Because our results further support the previous notion that membrane association is a general prerequisite for a wide range of Nef functions, the question arises of why Nef evolved to asso-

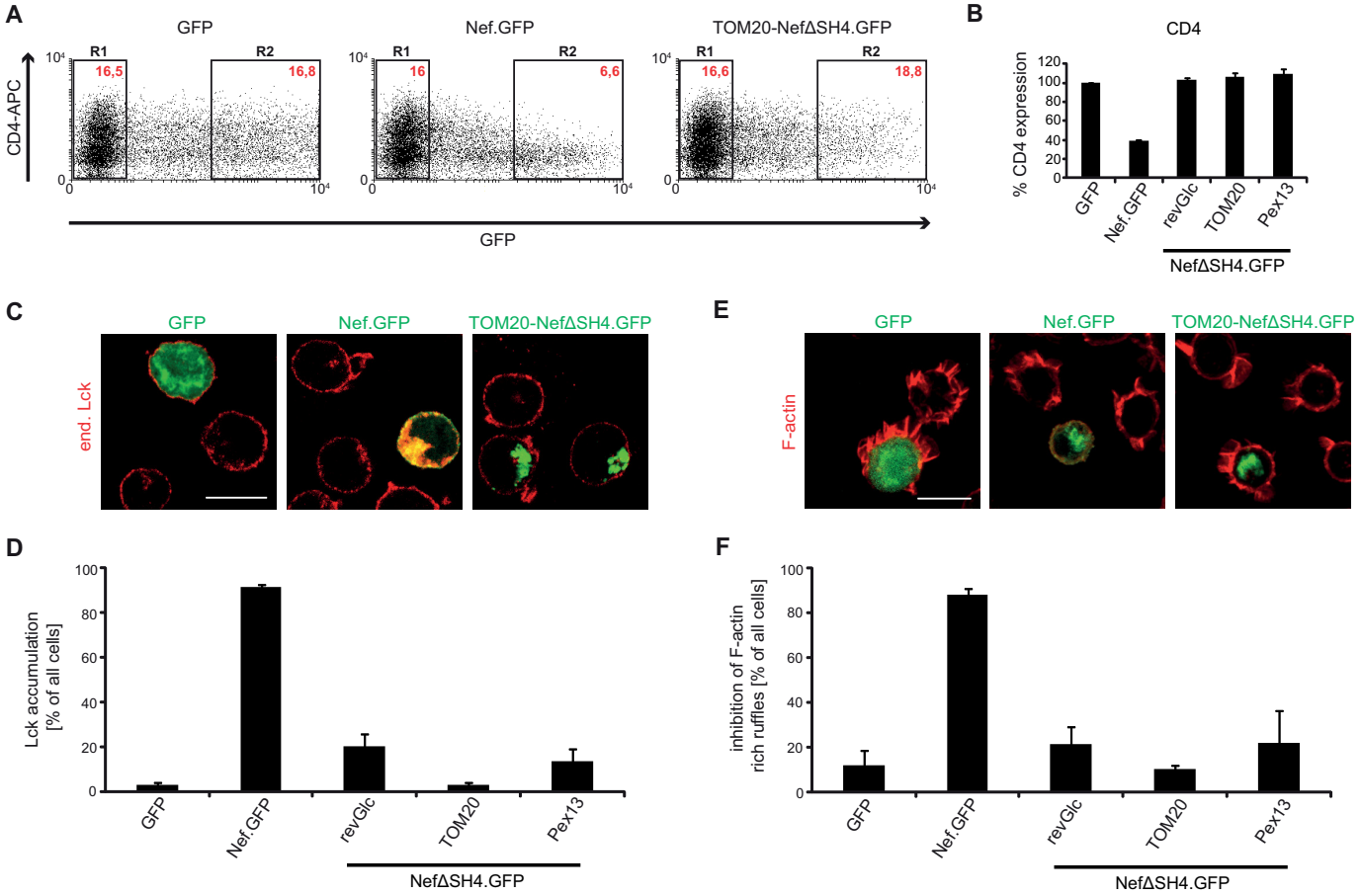

FIGURE 7. **Functional characterization of OT chimeric Nef.GFP proteins: down-regulation of cell surface CD4, Lck retargeting, and inhibition of F-actin ruffling.** *A*, CD4 cell surface expression in Jurkat TAg cells transfected with expression constructs for GFP, Nef.GFP, or TOM20-NefΔSH4.GFP. Twenty-four hours post-transfection, cells were stained for surface expression with allophycocyanin (*APC*)-conjugated antibodies against hm CD4 and analyzed by flow cytometry. *R1*, GFP-negative cells; *R2*, high level GFP expressing cells. *Red text*, MFIs of cells stained for CD4. *B*, down-regulation activity of the different OT Nef.GFP proteins. CD4 surface levels of GFP transfected cells were set to 100%. The data are means ± S.D. of at least three independent experiments. *C*, representative confocal pictures of Jurkat TAg cells transfected with expression constructs for GFP, Nef.GFP, or TOM20-NefΔSH4.GFP. The cells were plated on poly-L-lysine-coated cover glasses, fixed, and stained. Shown is a merge of endogenous (*end.*) Lck (*red*) and GFP (*green*). *Scale bar*, 10 μm. *D*, quantification of the frequency of cells displaying pronounced intracellular Lck accumulation. The data represent average values from three independent experiments ± S.D. with at least 100 cells analyzed per condition. *E*, representative maximum projections of confocal Z stacks of Jurkat CCR7 T cells transfected with expression constructs for GFP, Nef.GFP, or TOM20-NefΔSH4.GFP. Cells were plated on poly-L-lysine-coated cover glasses, stimulated with hm SDF-1α, fixed, and stained for F-actin using phalloidin-TRITC. Shown is the merge of F-actin (*red*) and GFP (*green*). *Scale bar*, 10 μm. *F*, quantification of cells that show full inhibition of F-actin ruffling. The data represent average values from three independent experiments ± S.D. with at least 100 cells analyzed per condition.

ciate with membranes with the low affinity provided by a myristoylated SH4 domain. Most SH4 domains of cellular proteins carry an additional fatty acid membrane anchor such as a palmitoyl moiety, which results in significantly more robust membrane anchoring. Enhancing the membrane affinity of Nef would only require one amino acid exchange (*e.g.* GC3 as in the PalmNef construct used here); however, such a mutation has not yet been observed in any primary HIV-1 isolate and thus is highly unlikely to provide a selective advantage for the virus in the infected host. One hypothesis that reconciles why Nef requires low affinity membrane association is that Nef function requires transient membrane interactions with high on/off rates. Even though we did not determine precise membrane affinities and membrane residence times, the magnitude of steady state membrane association and thus likely their time span of membrane association widely differed between the various SH4-Nef chimeras analyzed. The fact that all these constructs were similarly active in a broad range of biological activities suggests that the efficiency with which Nef dissociates from membranes is not limiting for Nef activity. Rather, membrane association *per se* irrespective of its duration appears to provide an essential cue for Nef function. As suggested earlier and supported by first experimental data very recently, this likely reflects a structural reorganization from a closed to an open conformation Nef undergoes upon membrane insertion (71, 72). In this scenario, membrane association enables Nef to undergo interactions with host cell proteins that likely stabilize Nef membrane association, whereas the cytoplasmic majority of Nef molecules per cell is inactive. On the other hand, this predicts that prolonged membrane association of Nef can lead to elevated biological activity in scenarios in which the amounts of Nef available for membrane interactions are limiting. This may be particularly relevant in infected primary T lymphocytes in which the efficacy of HIV-1 replication is a result of a balance between cell permissivity to infection and prevention of activation-induced cell death (15). Adverse effects on cell survival and thus virus spread exerted by T cell hyperactivation induced by efficiently membrane-associated Nef may thus explain why

evolution selects against a more potent membrane anchor of Nef.

Another central result of this study was that the anterograde transport route and the specific membrane microdomain environment used for PM delivery do not impact on the biological activity of Nef. Given that (i) effects of Nef such as down-modulation of MHC-I molecules from the cell surface or retargeting of Lck from the plasma membrane to recycling endosome/TGN compartments involve the inhibition of the anterograde transport of these molecules and (ii) Nef seems to interfere with intracellular transport of a specific subset of membrane microdomains (24), this result was surprising at first. However, this is consistent with our previous findings that microdomain association of Nef itself as well as physical association or colocalization with Lck is dispensable for interference with anterograde transport of the kinase (16, 22, 24). Together these results predict that Nef affects Lck anterograde transport via an indirect mechanism that can be exerted at a distance. In contrast, MHC-I down-regulation from the cell surface is thought to reflect sequestration of newly synthesized MHC-I molecules by a Nef AP-1 (adaptor protein 1) complex at the TGN prior to anterograde transport to the PM (63). Conceivably, segregation of transport pathways targeted by different SH4 domains occurs at a post-TGN sorting step, and AP-1 can be recruited by Nef irrespective of its local membrane microenvironment, explaining why differential SH4 domain membrane targeting did not alter this Nef activity (data not shown). Such independence of the specific anterograde transport route could also explain the activity of Nef fusion proteins with transmembrane and extracellular domains of surface receptors (CD4 or CD8) in signal transduction and vesicular transport (27, 57, 73–78), which are delivered to the PM by the classical secretory pathway that is clearly distinct from the less well characterized PM delivery routes used by SH4 domain-containing proteins (54, 60, 79–83).

Although heterologous SH4 domain targeting did not affect the biological properties of Nef, the OT Nef proteins entirely lacked activity in all functions tested. Because the topology of Nef as peripheral membrane protein exposed to the cytoplasm was preserved in these OT Nef proteins, this result illustrates that the action of membrane-associated Nef cannot be simply explained by the recruitment of cytoplasmic factors and assigns an important role to the nature of the host cell membrane Nef associates to. In this context the observed loss of function is particularly surprising for revGlc-NefΔSH4.GFP because it targets Nef to the cytoplasmic surface of the Golgi and thus in close proximity to the proposed site of action (TGN) for various Nef activities. If not the specific site of their localization, which characteristic could explain the functional difference between OT and SH4 domain-containing Nef.GFP proteins? One striking difference is that all SH4 domain-containing proteins were delivered to the PM, albeit with varying speed and efficiency, prior to subsequent sorting to their steady state destination. In contrast, all OT Nef.GFP proteins reached their destination without displaying detectable PM localization (data not shown). Our data are therefore consistent with the idea that the PM is the exclusive subcellular site of Nef activity irrespective of the transport route used. As discussed above, however, at least some Nef activities, such as MHC-I down-regulation, rely on physical association of Nef with cargo molecules during anterograde transport and thus likely prior to PM delivery. We therefore favor the hypothesis that the differential activity of OT and SH4 domain constructs is determined by the dynamics of their intracellular distribution. This interpretation is in line with a model introduced by Arold and Baur (71), according to which Nef function depends on "cycles" of the viral protein through biosynthetic and endocytic sorting steps. In this scenario, membrane-associated Nef could undergo sequential protein interactions, which might explain how the viral protein can exert so many seemingly independent functions. Because Nef exerts these activities in the course of the cycle, the steady state localization, which reflects the final and rate-limiting transport step, does not necessarily indicate its biological activity.

The machinery mediating anterograde transport of Nef remains to be identified. Although this might involve traditional vesicular transport routes, the abundance of non-membrane-associated Nef protein in the cytoplasm could also allow for direct recruitment of Nef to target membranes from this soluble pool. Unlike other myristoylated proteins, Nef does not undergo induced triggered conformational changes (myristol switch (84)) that could regulate such membrane recruitment. The preference of Nef for binding to highly curved membranes (40) suggests that Nef is far more likely to attach to small transport vesicles than to the less curved PM. We therefore propose that PM delivery, from soluble cytoplasmic pools or via anterograde transport, involves specific transport vesicles to which Nef remains stably attached. Once delivered to target membranes such as the PM, the reduced curvature may result in membrane dissociation of Nef unless membrane attachment is stabilized by specific protein interactions.

Together, our results suggest that the mechanisms governing dynamic membrane interactions of Nef are far more complex than previously anticipated and central for the regulation of its biological properties. Critical open questions include at which specific subcellular sites Nef exerts its individual functions, which cues regulate Nef membrane association and which transport machinery delivers Nef to the PM. To address these issues, several technical challenges will need to be overcome to visualize the biosynthetic transport of Nef and to specifically disrupt the transport machinery involved. Beyond its critical role in AIDS pathogenesis, Nef will continue to serve as a valuable model system for studies of intracellular transport routes for peripheral membrane proteins.

REFERENCES

1. Deacon, N. J., Tsykin, A., Solomon, A., Smith, K., Ludford-Menting, M., Hooker, D. J., McPhee, D. A., Greenway, A. L., Ellett, A., Chatfield, C., Lawson, V. A., Crowe, S., Maerz, A., Sonza, S., Learmont, J., Sullivan, J. S., Cunningham, A., Dwyer, D., Dowton, D., and Mills, J. (1995) Genomic structure of an attenuated quasi species of HIV-1 from a blood transfusion donor and recipients. *Science* **270,** 988–991
2. Kestler, H. W., 3rd, Ringler, D. J., Mori, K., Panicali, D. L., Sehgal, P. K., Daniel, M. D., and Desrosiers, R. C. (1991) Importance of the nef gene for maintenance of high virus loads and for development of AIDS. *Cell* **65,** 651–662
3. Kirchhoff, F., Greenough, T. C., Brettler, D. B., Sullivan, J. L., and Desrosiers, R. C. (1995) Brief report: absence of intact nef sequences in a long-term survivor with nonprogressive HIV-1 infection. *N. Engl. J. Med.* **332,**

228–232
4. Hanna, Z., Kay, D. G., Rebai, N., Guimond, A., Jothy, S., and Jolicoeur, P. (1998) Nef harbors a major determinant of pathogenicity for an AIDS-like disease induced by HIV-1 in transgenic mice. *Cell* **95,** 163–175
5. Rahim, M. M., Chrobak, P., Hu, C., Hanna, Z., and Jolicoeur, P. (2009) Adult AIDS-like disease in a novel inducible human immunodeficiency virus type 1 Nef transgenic mouse model: CD4+ T-cell activation is Nef dependent and can occur in the absence of lymphophenia. *J. Virol.* **83,** 11830–11846
6. Garcia, J. V., and Miller, A. D. (1991) Serine phosphorylation-independent downregulation of cell-surface CD4 by nef. *Nature* **350,** 508–511
7. Michel, N., Allespach, I., Venzke, S., Fackler, O. T., and Keppler, O. T. (2005) The Nef protein of human immunodeficiency virus establishes superinfection immunity by a dual strategy to downregulate cell-surface CCR5 and CD4. *Curr. Biol.* **15,** 714–723
8. Collins, K. L., Chen, B. K., Kalams, S. A., Walker, B. D., and Baltimore, D. (1998) HIV-1 Nef protein protects infected primary cells against killing by cytotoxic T lymphocytes. *Nature* **391,** 397–401
9. Schwartz, O., Maréchal, V., Le Gall, S., Lemonnier, F., and Heard, J. M. (1996) Endocytosis of major histocompatibility complex class I molecules is induced by the HIV-1 Nef protein. *Nat. Med.* **2,** 338–342
10. Aiken, C., and Trono, D. (1995) Nef stimulates human immunodeficiency virus type 1 proviral DNA synthesis. *J. Virol.* **69,** 5048–5056
11. Chowers, M. Y., Spina, C. A., Kwoh, T. J., Fitch, N. J., Richman, D. D., and Guatelli, J. C. (1994) Optimal infectivity in vitro of human immunodeficiency virus type 1 requires an intact nef gene. *J. Virol.* **68,** 2906–2914
12. Lama, J., Mangasarian, A., and Trono, D. (1999) Cell-surface expression of CD4 reduces HIV-1 infectivity by blocking Env incorporation in a Nef- and Vpu-inhibitable manner. *Curr. Biol.* **9,** 622–631
13. Schwartz, O., Maréchal, V., Danos, O., and Heard, J. M. (1995) Human immunodeficiency virus type 1 Nef increases the efficiency of reverse transcription in the infected cell. *J. Virol.* **69,** 4053–4059
14. Abraham, L., Bankhead, P., Pan, X., Engel, U., and Fackler, O. T. (2012) HIV-1 Nef limits communication between linker of activated T cells and SLP-76 to reduce formation of SLP-76-signaling microclusters following TCR stimulation. *J. Immunol.* **189,** 1898–1910
15. Abraham, L., and Fackler, O. T. (2012) HIV-1 Nef: a multifaceted modulator of T cell receptor signaling. *Cell Commun. Signal.* **10,** 39
16. Pan, X., Rudolph, J. M., Abraham, L., Habermann, A., Haller, C., Krijnse-Locker, J., and Fackler, O. T. (2012) HIV-1 Nef compensates for disorganization of the immunological synapse by inducing *trans*-Golgi network-associated Lck signaling. *Blood* **119,** 786–797
17. Schrager, J. A., and Marsh, J. W. (1999) HIV-1 Nef increases T cell activation in a stimulus-dependent manner. *Proc. Natl. Acad. Sci. U.S.A.* **96,** 8167–8172
18. Stolp, B., Abraham, L., Rudolph, J. M., and Fackler, O. T. (2010) Lentiviral Nef proteins utilize PAK2-mediated deregulation of cofilin as a general strategy to interfere with actin remodeling. *J. Virol.* **84,** 3935–3948
19. Stolp, B., Reichman-Fried, M., Abraham, L., Pan, X., Giese, S. I., Hannemann, S., Goulimari, P., Raz, E., Grosse, R., and Fackler, O. T. (2009) HIV-1 Nef interferes with host cell motility by deregulation of Cofilin. *Cell Host Microbe* **6,** 174–186
20. Thoulouze, M. I., Sol-Foulon, N., Blanchet, F., Dautry-Varsat, A., Schwartz, O., and Alcover, A. (2006) Human immunodeficiency virus type-1 infection impairs the formation of the immunological synapse. *Immunity* **24,** 547–561
21. Arhel, N., Lehmann, M., Clauss, K., Nienhaus, G. U., Piguet, V., and Kirchhoff, F. (2009) The inability to disrupt the immunological synapse between infected human T cells and APCs distinguishes HIV-1 from most other primate lentiviruses. *J. Clin. Invest.* **119,** 2965–2975
22. Haller, C., Rauch, S., and Fackler, O. T. (2007) HIV-1 Nef employs two distinct mechanisms to modulate Lck subcellular localization and TCR induced actin remodeling. *PLoS One* **2,** e1212
23. Haller, C., Rauch, S., Michel, N., Hannemann, S., Lehmann, M. J., Keppler, O. T., and Fackler, O. T. (2006) The HIV-1 pathogenicity factor Nef interferes with maturation of stimulatory T-lymphocyte contacts by modulation of N-Wasp activity. *J. Biol. Chem.* **281,** 19618–19630
24. Pan, X., Geist, M. M., Rudolph, J. M., Nickel, W., and Fackler, O. T. (2013) HIV-1 Nef disrupts membrane-microdomain-associated anterograde transport for plasma membrane delivery of selected Src family kinases. *Cell. Microbiol.* **15,** 1605–1621
25. Rudolph, J. M., Eickel, N., Haller, C., Schindler, M., and Fackler, O. T. (2009) Inhibition of T-cell receptor-induced actin remodeling and relocalization of Lck are evolutionarily conserved activities of lentiviral Nef proteins. *J. Virol.* **83,** 11528–11539
26. Schindler, M., Münch, J., Kutsch, O., Li, H., Santiago, M. L., Bibollet-Ruche, F., Müller-Trutwin, M. C., Novembre, F. J., Peeters, M., Courgnaud, V., Bailes, E., Roques, P., Sodora, D. L., Silvestri, G., Sharp, P. M., Hahn, B. H., and Kirchhoff, F. (2006) Nef-mediated suppression of T cell activation was lost in a lentiviral lineage that gave rise to HIV-1. *Cell* **125,** 1055–1067
27. Aiken, C., Konner, J., Landau, N. R., Lenburg, M. E., and Trono, D. (1994) Nef induces CD4 endocytosis: requirement for a critical dileucine motif in the membrane-proximal CD4 cytoplasmic domain. *Cell* **76,** 853–864
28. Bentham, M., Mazaleyrat, S., and Harris, M. (2006) Role of myristoylation and N-terminal basic residues in membrane association of the human immunodeficiency virus type 1 Nef protein. *J. Gen. Virol.* **87,** 563–571
29. Fackler, O. T., Moris, A., Tibroni, N., Giese, S. I., Glass, B., Schwartz, O., and Kräusslich, H. G. (2006) Functional characterization of HIV-1 Nef mutants in the context of viral infection. *Virology* **351,** 322–339
30. Giese, S. I., Woerz, I., Homann, S., Tibroni, N., Geyer, M., and Fackler, O. T. (2006) Specific and distinct determinants mediate membrane binding and lipid raft incorporation of HIV-1(SF2) Nef. *Virology* **355,** 175–191
31. Goldsmith, M. A., Warmerdam, M. T., Atchison, R. E., Miller, M. D., and Greene, W. C. (1995) Dissociation of the CD4 downregulation and viral infectivity enhancement functions of human immunodeficiency virus type 1 Nef. *J. Virol.* **69,** 4112–4121
32. Sawai, E. T., Baur, A. S., Peterlin, B. M., Levy, J. A., and Cheng-Mayer, C. (1995) A conserved domain and membrane targeting of Nef from HIV and SIV are required for association with a cellular serine kinase activity. *J. Biol. Chem.* **270,** 15307–15314
33. Franchini, G., Robert-Guroff, M., Ghrayeb, J., Chang, N. T., and Wong-Staal, F. (1986) Cytoplasmic localization of the HTLV-III 3′ orf protein in cultured T cells. *Virology* **155,** 593–599
34. Guy, B., Kieny, M. P., Riviere, Y., Le Peuch, C., Dott, K., Girard, M., Montagnier, L., and Lecocq, J. P. (1987) HIV F/3′ orf encodes a phosphorylated GTP-binding protein resembling an oncogene product. *Nature* **330,** 266–269
35. Kaminchik, J., Bashan, N., Itach, A., Sarver, N., Gorecki, M., and Panet, A. (1991) Genetic characterization of human immunodeficiency virus type 1 nef gene products translated in vitro and expressed in mammalian cells. *J. Virol.* **65,** 583–588
36. Kaminchik, J., Margalit, R., Yaish, S., Drummer, H., Amit, B., Sarver, N., Gorecki, M., and Panet, A. (1994) Cellular distribution of HIV type 1 Nef protein: identification of domains in Nef required for association with membrane and detergent-insoluble cellular matrix. *AIDS Res. Hum. Retroviruses* **10,** 1003–1010
37. Peitzsch, R. M., and McLaughlin, S. (1993) Binding of acylated peptides and fatty acids to phospholipid vesicles: pertinence to myristoylated proteins. *Biochemistry* **32,** 10436–10443
38. Resh, M. D. (1999) Fatty acylation of proteins: new insights into membrane targeting of myristoylated and palmitoylated proteins. *Biochim. Biophys. Acta* **1451,** 1–16
39. Welker, R., Harris, M., Cardel, B., and Kräusslich, H. G. (1998) Virion incorporation of human immunodeficiency virus type 1 Nef is mediated by a bipartite membrane-targeting signal: analysis of its role in enhancement of viral infectivity. *J. Virol.* **72,** 8833–8840
40. Gerlach, H., Laumann, V., Martens, S., Becker, C. F., Goody, R. S., and Geyer, M. (2010) HIV-1 Nef membrane association depends on charge, curvature, composition and sequence. *Nat. Chem. Biol.* **6,** 46–53
41. Aldrovandi, G. M., Gao, L., Bristol, G., and Zack, J. A. (1998) Regions of human immunodeficiency virus type 1 nef required for function *in vivo*. *J. Virol.* **72,** 7032–7039
42. Geyer, M., Fackler, O. T., and Peterlin, B. M. (2001) Structure-function relationships in HIV-1 Nef. *EMBO Rep.* **2,** 580–585
43. Peng, B., and Robert-Guroff, M. (2001) Deletion of N-terminal myristoy-

lation site of HIV Nef abrogates both MHC-1 and CD4 down-regulation. *Immunol. Lett.* **78,** 195–200
44. Zazopoulos, E., and Haseltine, W. A. (1992) Mutational analysis of the human immunodeficiency virus type 1 Eli Nef function. *Proc. Natl. Acad. Sci. U.S.A.* **89,** 6634–6638
45. Fackler, O. T., Luo, W., Geyer, M., Alberts, A. S., and Peterlin, B. M. (1999) Activation of Vav by Nef induces cytoskeletal rearrangements and downstream effector functions. *Mol. Cell* **3,** 729–739
46. Northrop, J. P., Ullman, K. S., and Crabtree, G. R. (1993) Characterization of the nuclear and cytoplasmic components of the lymphoid-specific nuclear factor of activated T cells (NF-AT) complex. *J. Biol. Chem.* **268,** 2917–2923
47. Pevzner, I., Strating, J., Lifshitz, L., Parnis, A., Glaser, F., Herrmann, A., Brügger, B., Wieland, F., and Cassel, D. (2012) Distinct role of subcomplexes of the COPI coat in the regulation of ArfGAP2 activity. *Traffic* **13,** 849–856
48. Krautkrämer, E., Giese, S. I., Gasteier, J. E., Muranyi, W., and Fackler, O. T. (2004) Human immunodeficiency virus type 1 Nef activates p21-activated kinase via recruitment into lipid rafts. *J. Virol.* **78,** 4085–4097
49. Fransen, M., Wylin, T., Brees, C., Mannaerts, G. P., and Van Veldhoven, P. P. (2001) Human pex19p binds peroxisomal integral membrane proteins at regions distinct from their sorting sequences. *Mol. Cell. Biol.* **21,** 4413–4424
50. Sharpe, H. J., Stevens, T. J., and Munro, S. (2010) A comprehensive comparison of transmembrane domains reveals organelle-specific properties. *Cell* **142,** 158–169
51. Keppler, O. T., Tibroni, N., Venzke, S., Rauch, S., and Fackler, O. T. (2006) Modulation of specific surface receptors and activation sensitization in primary resting CD4+ T lymphocytes by the Nef protein of HIV-1. *J. Leukocyte Biol.* **79,** 616–627
52. Stolp, B., Imle, A., Coelho, F. M., Hons, M., Gorina, R., Lyck, R., Stein, J. V., and Fackler, O. T. (2012) HIV-1 Nef interferes with T-lymphocyte circulation through confined environments in vivo. *Proc. Natl. Acad. Sci. U.S.A.* **109,** 18541–18546
53. Schmidt, S., Fritz, J. V., Bitzegeio, J., Fackler, O. T., and Keppler, O. T. (2011) HIV-1 Vpu blocks recycling and biosynthetic transport of the intrinsic immunity factor CD317/tetherin to overcome the virion release restriction. *mBio* **2,** e00036–00011
54. Tournaviti, S., Pietro, E. S., Terjung, S., Schafmeier, T., Wegehingel, S., Ritzerfeld, J., Schulz, J., Smith, D. F., Pepperkok, R., and Nickel, W. (2009) Reversible phosphorylation as a molecular switch to regulate plasma membrane targeting of acylated SH4 domain proteins. *Traffic* **10,** 1047–1060
55. Sol-Foulon, N., Esnault, C., Percherancier, Y., Porrot, F., Metais-Cunha, P., Bachelerie, F., and Schwartz, O. (2004) The effects of HIV-1 Nef on CD4 surface expression and viral infectivity in lymphoid cells are independent of rafts. *J. Biol. Chem.* **279,** 31398–31408
56. Greenberg, M. E., Bronson, S., Lock, M., Neumann, M., Pavlakis, G. N., and Skowronski, J. (1997) Co-localization of HIV-1 Nef with the AP-2 adaptor protein complex correlates with Nef-induced CD4 down-regulation. *EMBO J.* **16,** 6964–6976
57. Madrid, R., Janvier, K., Hitchin, D., Day, J., Coleman, S., Noviello, C., Bouchet, J., Benmerah, A., Guatelli, J., and Benichou, S. (2005) Nef-induced alteration of the early/recycling endosomal compartment correlates with enhancement of HIV-1 infectivity. *J. Biol. Chem.* **280,** 5032–5044
58. Alexander, M., Bor, Y. C., Ravichandran, K. S., Hammarskjöld, M. L., and Rekosh, D. (2004) Human immunodeficiency virus type 1 Nef associates with lipid rafts to downmodulate cell surface CD4 and class I major histocompatibility complex expression and to increase viral infectivity. *J. Virol.* **78,** 1685–1696
59. Coates, K., Cooke, S. J., Mann, D. A., and Harris, M. P. (1997) Protein kinase C-mediated phosphorylation of HIV-I nef in human cell lines. *J. Biol. Chem.* **272,** 12289–12294
60. Sato, I., Obata, Y., Kasahara, K., Nakayama, Y., Fukumoto, Y., Yamasaki, T., Yokoyama, K. K., Saito, T., and Yamaguchi, N. (2009) Differential trafficking of Src, Lyn, Yes and Fyn is specified by the state of palmitoylation in the SH4 domain. *J. Cell Sci.* **122,** 965–975
61. Akari, H., Arold, S., Fukumori, T., Okazaki, T., Strebel, K., and Adachi, A. (2000) Nef-induced major histocompatibility complex class I down-regulation is functionally dissociated from its virion incorporation, enhancement of viral infectivity, and CD4 down-regulation. *J. Virol.* **74,** 2907–2912
62. Blagoveshchenskaya, A. D., Thomas, L., Feliciangeli, S. F., Hung, C. H., and Thomas, G. (2002) HIV-1 Nef downregulates MHC-I by a PACS-1- and PI3K-regulated ARF6 endocytic pathway. *Cell* **111,** 853–866
63. Jia, X., Singh, R., Homann, S., Yang, H., Guatelli, J., and Xiong, Y. (2012) Structural basis of evasion of cellular adaptive immunity by HIV-1 Nef. *Nat. Struct. Mol. Biol.* **19,** 701–706
64. Noviello, C. M., Benichou, S., and Guatelli, J. C. (2008) Cooperative binding of the class I major histocompatibility complex cytoplasmic domain and human immunodeficiency virus type 1 Nef to the endosomal AP-1 complex via its mu subunit. *J. Virol.* **82,** 1249–1258
65. Wonderlich, E. R., Williams, M., and Collins, K. L. (2008) The tyrosine binding pocket in the adaptor protein 1 (AP-1) mu1 subunit is necessary for Nef to recruit AP-1 to the major histocompatibility complex class I cytoplasmic tail. *J. Biol. Chem.* **283,** 3011–3022
66. Mossalam, M., Matissek, K. J., Okal, A., Constance, J. E., and Lim, C. S. (2012) Direct induction of apoptosis using an optimal mitochondrially targeted p53. *Mol. Pharm.* **9,** 1449–1458
67. Suzuki, H., Maeda, M., and Mihara, K. (2002) Characterization of rat TOM70 as a receptor of the preprotein translocase of the mitochondrial outer membrane. *J. Cell Sci.* **115,** 1895–1905
68. Laguette, N., Brégnard, C., Bouchet, J., Benmerah, A., Benichou, S., and Basmaciogullari, S. (2009) Nef-induced CD4 endocytosis in human immunodeficiency virus type 1 host cells: role of p56lck kinase. *J. Virol.* **83,** 7117–7128
69. Tokarev, A., and Guatelli, J. (2011) Misdirection of membrane trafficking by HIV-1 Vpu and Nef: Keys to viral virulence and persistence. *Cell. Logist.* **1,** 90–102
70. Wolf, D., Witte, V., Clark, P., Blume, K., Lichtenheld, M. G., and Baur, A. S. (2008) HIV Nef enhances Tat-mediated viral transcription through a hnRNP-K-nucleated signaling complex. *Cell Host Microbe* **4,** 398–408
71. Arold, S. T., and Baur, A. S. (2001) Dynamic Nef and Nef dynamics: how structure could explain the complex activities of this small HIV protein. *Trends Biochem. Sci.* **26,** 356–363
72. Akgun, B., Satija, S., Nanda, H., Pirrone, G. F., Shi, X., Engen, J. R., and Kent, M. S. (2013) Conformational transition of membrane-associated terminally acylated HIV-1 Nef. *Structure* **21,** 1822–1833
73. Baur, A. S., Sass, G., Laffert, B., Willbold, D., Cheng-Mayer, C., and Peterlin, B. M. (1997) The N-terminus of Nef from HIV-1/SIV associates with a protein complex containing Lck and a serine kinase. *Immunity* **6,** 283–291
74. Baur, A. S., Sawai, E. T., Dazin, P., Fantl, W. J., Cheng-Mayer, C., and Peterlin, B. M. (1994) HIV-1 Nef leads to inhibition or activation of T cells depending on its intracellular localization. *Immunity* **1,** 373–384
75. Bresnahan, P. A., Yonemoto, W., Ferrell, S., Williams-Herman, D., Geleziunas, R., and Greene, W. C. (1998) A dileucine motif in HIV-1 Nef acts as an internalization signal for CD4 downregulation and binds the AP-1 clathrin adaptor. *Curr. Biol.* **8,** 1235–1238
76. Mangasarian, A., Foti, M., Aiken, C., Chin, D., Carpentier, J. L., and Trono, D. (1997) The HIV-1 Nef protein acts as a connector with sorting pathways in the Golgi and at the plasma membrane. *Immunity* **6,** 67–77
77. Witte, V., Laffert, B., Gintschel, P., Krautkrämer, E., Blume, K., Fackler, O. T., and Baur, A. S. (2008) Induction of HIV transcription by Nef involves Lck activation and protein kinase Cθ raft recruitment leading to activation of ERK1/2 but not NFκB. *J. Immunol.* **181,** 8425–8432
78. Xu, X. N., Laffert, B., Screaton, G. R., Kraft, M., Wolf, D., Kolanus, W., Mongkolsapay, J., McMichael, A. J., and Baur, A. S. (1999) Induction of Fas ligand expression by HIV involves the interaction of Nef with the T cell receptor ζ chain. *J. Exp. Med.* **189,** 1489–1496
79. Kasahara, K., Nakayama, Y., Ikeda, K., Fukushima, Y., Matsuda, D., Horimoto, S., and Yamaguchi, N. (2004) Trafficking of Lyn through the Golgi caveolin involves the charged residues on αE and αI helices in the kinase domain. *J. Cell Biol.* **165,** 641–652
80. Kasahara, K., Nakayama, Y., Kihara, A., Matsuda, D., Ikeda, K., Kuga, T., Fukumoto, Y., Igarashi, Y., and Yamaguchi, N. (2007) Rapid trafficking of

c-Src, a non-palmitoylated Src-family kinase, between the plasma membrane and late endosomes/lysosomes. *Exp. Cell Res.* **313,** 2651–2666
81. Nickel, W. (2005) Unconventional secretory routes: direct protein export across the plasma membrane of mammalian cells. *Traffic* **6,** 607–614
82. Ritzerfeld, J., Remmele, S., Wang, T., Temmerman, K., Brügger, B., Wegehingel, S., Tournaviti, S., Strating, J. R., Wieland, F. T., Neumann, B., Ellenberg, J., Lawerenz, C., Hesser, J., Erfle, H., Pepperkok, R., and Nickel, W. (2011) Phenotypic profiling of the human genome reveals gene products involved in plasma membrane targeting of SRC kinases. *Genome Res.* **21,** 1955–1968
83. van't Hof, W., and Resh, M. D. (1997) Rapid plasma membrane anchoring of newly synthesized p59fyn: selective requirement for NH_2-terminal myristoylation and palmitoylation at cysteine-3. *J. Cell Biol.* **136,** 1023–1035
84. Morgan, C. R., Miglionico, B. V., and Engen, J. R. (2011) Effects of HIV-1 Nef on human *N*-myristoyltransferase 1. *Biochemistry* **50,** 3394–3403